Stochastic Design Optimization of Microstructural Features Using Linear Programming for Robust Design

Pinar Acar*

Virginia Polytechnic Institute and State University, Blacksburg, Virginia 24061

and

Veera Sundararaghavan[†]

University of Michigan, Ann Arbor, Michigan 48109

Microstructure design can have a substantial effect on the performance of critical components in numerous aerospace applications. However, the stochastic nature of metallic microstructures leads to deviations in material properties from the design point and alters the performance of these critical components. In this paper, a novel stochastic linear programming (LP) methodology is developed for microstructure design accounting for uncertainties in desired properties. The metallic microstructure is represented using a finite element discretized form of the orientation distribution function (ODF). The inverse LP problem solves the mean values and covariance matrix of the ODFs to maximize the mean values of a property, given the statistical constraints on other properties. The highlight is an analytical uncertainty quantification model via a Gaussian distribution to model propagation of microstructural uncertainties to the properties. Examples illustrate maximization of the yield strength and magnetostriction of a galfenol alloy when constrained by uncertainties in a set of stiffness constants.

Nomenclature

A	=	orientation distribution function
C	=	stiffness
E	=	expected value
m	=	property vector for magnetostrictive strain
p	=	property matrix for stiffness
q	=	volume normalization vector
V	=	null space vector
y	=	property vector for yield stress
μ_A	=	mean value of the orientation distribution function
μ_C	=	mean value of the stiffness
Σ_A	=	variance of the orientation distribution function
Σ_C	=	variance of the stiffness

I. Introduction

MICROSTRUCTURE design has been typically addressed as a deterministic optimization problem in which features such as volume fractions of various phases are controlled to achieve the desired property. Several issues arise: First, multiple microstructures can lead to the desired property, and some microstructures are easier to manufacture than others [1,2]. Thus, the deterministic optimizer has to be capable of predicting nonunique solutions. Second, manufacturing process conditions create uncertainties in microstructural features. This is an aleatoric uncertainty, is unavoidable, and is naturally present in metallic systems. Thus, the final realized material has variability in properties around the design endpoint. Although small variability is acceptable, larger variabilities can often lead to severe performance issues. For example, unfavorable crystallographic texture in a polycrystalline alloy can create weaknesses that can initiate fracture [3].

The current state of the art mostly addresses the direct uncertainty quantification (UQ) problem, i.e., prediction of the effect of

microstructural uncertainty on properties. The direct problem has been generally addressed using computational techniques such as the Monte Carlo simulation (MCS), collocation, and spectral decomposition methods. Huyse and Maes [4] studied the effect of microstructural uncertainties on homogenized parameters by using random windows from the real microstructure, and they performed a MCS to identify the stochasticity in elastic parameters such as Young's modulus and Poisson's ratio. Sakata et al. [5] showed the variations in Young's modulus and Poisson's ratio due to microscopic uncertainties. They validated the results of their perturbation-based homogenization method with the MCS. In another paper, Sakata et al. [6] implemented a kriging approach to calculate the probability density functions of the material properties and used the MCS to study the uncertainties in geometry and the material properties of a microstructure through the same perturbation-based homogenization method. A computational stochastic modeling approach for random microstructure geometry was presented by Clement et al. [7,8]. The authors presented a high-dimensional problem due to the high number of stochastic variables to represent the microstructure geometry. This high-dimensionality was reduced with the implementation of polynomial chaos expansion. Creuziger et al. [9] examined the uncertainties in the orientation distribution function (ODF) values of a microstructure due to the variations in the pole figure values by using the MCS. Juan et al. [10] used the MCS to study the effects of a sampling strategy on the determination of various characteristic microstructure parameters such as grain size distribution and grain topology distribution. Hiriyur et al. [11] studied an extended finite element method coupled with an MCS approach to quantify the uncertainties in the homogenized effective elastic properties of multiphase materials. The uncertain parameters were assumed to be aspect ratios, spatial distribution, and orientation. They used a strain energy approach to analyze the uncertainties of an in-plane Young's modulus and Poisson's ratio. Kouchmeshky and Zabaras [12] presented the propagation of initial texture and deformation process uncertainties on the final product properties. They used a data-driven approach to identify the joint probability distributions of random variables with a maximum entropy method, and they modeled the stochastic problem using a stochastic collocation approach. Madrid et al. [13] examined the variability and sensitivity of an in-plane Young's modulus of thin nickel polycrystalline films due to uncertainties in the microstructure geometry, crystallographic texture, and numerical values of single crystal elastic constants by using a numerical spectral technique. Niezgoda et al. [14] computed the variances of the microstructure

properties by defining a stochastic process to represent the microstructure. In Ref. [15], the uncertainty in properties was estimated numerically using maximum information entropy given the known average grain size and texture.

Traditional numerical techniques, such as the MCS, are robust but computationally expensive [16]. In addition, these methods are generally able to represent the small variations in properties [17–21]. These UQ techniques studied in the literature also required high computational costs because they represented the joint probability distributions of the random variables using either interpolation functions or samples. As the problem complexity or the number of variables increased, the number of interpolation terms or sampling points also increased. This was especially true for the ODFs that were discretized using finite element nodes or a spectral basis, and they contained a large number of free parameters for which the joint distribution needed to be sampled. For computationally efficient simulations, the high-performance computing (HPC) could be considered for the solution. However, the HPC was not always optimal for the expense [22]. Thus, the materials community has recently focused on reduced-order modeling techniques. The most preferred method is proper orthogonal decomposition (POD) [1,23–27]. However, POD provides a linear formulation in the reduced basis, and it is better suited for linear or weakly nonlinear problems. All these disadvantages imply the necessity of developing analytical solutions as the first step in UQ. In our recent paper [28], we presented an analytical formulation based on multivariate Gaussian representation to model the variations in texture. Although this work propagated the uncertainty in the microstructure to the endpoint properties, the inverse problem was of specific interest in the paper. In the context of deterministic inverse problems, notable contributions include Refs. [29,30], in which the authors demonstrated texture design so as to maximize the elastic and plastic properties of a structure. Data-mining methods have been used for microstructure design in Refs. [31–33]. On the other hand, a survey of the literature revealed that the stochastic optimization problem for microstructure design has still not been addressed.

In this paper, we have developed a novel stochastic linear programming (LP) methodology for microstructure design. The inverse LP problem of the present work solves the mean values and the covariance matrix of the ODFs to maximize the mean values of a property, given statistical constraints on other properties. To the best of the authors' knowledge, this is the first stochastic microstructure optimization effort in the literature that can handle fully correlated ODFs. The organization of the paper is as follows: Section II addresses the multiscale modeling of microstructures: particularly, the computation of volume-averaged properties. The Gaussian random variables concept is introduced in Sec. III. We present the analytical model for UQ and the stochastic optimization approach using fully correlated random variables in Sec. IV. In Sec. V, we report the results of the stochastic optimization studies performed using the analytical algorithm to quantify the uncertainties. A summary of the paper with potential future applications is presented in Sec. VI.

II. Microstructure Representation

The alloy microstructure consists of multiple crystals with each crystal having an orientation. The generalized Hooke's law for the aggregate of crystals may be written in the following form:

$$\langle \boldsymbol{\sigma} \rangle = \boldsymbol{C}^{\text{eff}} \langle \boldsymbol{\epsilon} \rangle \tag{1}$$

where $\langle \boldsymbol{\epsilon} \rangle$ and $\langle \boldsymbol{\sigma} \rangle$ are the volume-averaged strain and stress, respectively; and $\boldsymbol{C}^{\text{eff}}$ is the effective stiffness tensor in the coordinate system of the part. Assuming homogeneity of the deformation in a macroscale elementary volume, the effective elastic constants may be found through averaging using the Taylor approximation [34]:

$$\boldsymbol{C}^{\text{eff}} = \langle \boldsymbol{C} \rangle \tag{2}$$

If the effect of factors (e.g., crystal size and shape) is ignored, averaging (denoted by $\langle \cdot \rangle$ in the preceding equation) can be performed over the ODF (represented by A). The ODF gives the
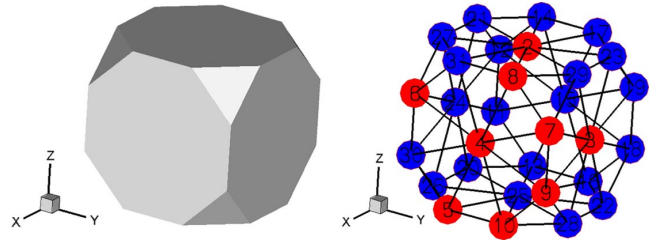

Fig. 1   ODF representation in the Rodrigues fundamental region for cubic crystal symmetry, showing the location of the $k = 10$ independent nodes of the ODF in red.

volume density of each orientation in the microstructure. If the orientation-dependent property for single crystals $\chi(\boldsymbol{r})$ is known, any polycrystal property can be expressed as an expected value, or average, given by the following:

$$\langle \chi \rangle = \int_R \chi(\boldsymbol{r}) A(\boldsymbol{r}) \, \mathrm{d}v \tag{3}$$

where the ODF A is a function of the crystal orientation $\boldsymbol{r}$. The average value is computed by integrating in the fundamental region R of the crystal orientation space, which can be obtained by considering crystallographic symmetries.

The present work employs the Rodrigues axis-angle parameterization of the crystal orientation space [35,36]. The Rodrigues parameterization is created by scaling the axis of rotation $\boldsymbol{n}$ as $\boldsymbol{r} = \boldsymbol{n} \tan(\theta/2)$, where θ is the rotation angle. The Rodrigues space is advantageous due to the regularity of its geometry [35], which allows us to discretize the space using finite elements. The ODF is discretized into N independent nodes with N_{elem} finite elements and N_{int} integration points per element. A finite element integration scheme using Gauss quadrature allows the matrix representation of Eq. (3). Using this parametrization, any polycrystal property can be expressed in a linear form as follows [37]:

$$\langle \chi \rangle = \int_R \chi(\boldsymbol{r}) A(\boldsymbol{r}) \, \mathrm{d}v = \sum_{n=1}^{N_{\text{elem}}} \sum_{m=1}^{N_{\text{int}}} \chi(r_m) A(r_m) w_m |J_n| \frac{1}{(1 + r_m \cdot r_m)^2} \tag{4}$$

where $A(r_m)$ is the value of the ODF at the mth integration point with global coordinate r_m of the nth element, $|J_n|$ is the Jacobian determinant of the nth element, w_m is the integration weight associated with the nth integration point, and $1/(1 + r_m \cdot r_m)^2$ represents the metric of Rodrigues parameterization. This can be shown to be equivalent to an equation linear in the ODF: $\langle \chi \rangle = p^T A$, where A is a column vector containing the ODF values at the k independent nodes of the ODF mesh [28]. In addition, the ODF is normalized to unity as $q^T A = 1$, where q is a normalization (column) vector. An example for the ODF representation for body-centered cubic (BCC) galfenol material is shown in Fig. 1.

III. Uncertainty Representation

The ODF is represented using a d-dimensional multivariate Gaussian distribution $A \sim N(\boldsymbol{\mu}_A, \boldsymbol{\Sigma}_A)$, where $\boldsymbol{\mu}_A$ is a vector of mean values of the ODF at independent nodes $\boldsymbol{\mu}_A = (\mu_1, \ldots, \mu_k)^T = E[A]$, and $\boldsymbol{\Sigma}_A$ is the covariance matrix $\Sigma_{A_{ij}} = \text{cov}(A_i, A_j) = E[(A_i - \mu_{A_i})(A_j - \mu_{A_j})]$, $i, j = 1, \ldots, k$. In our previous work [28], we showed that any property that is linearly related to the ODF (e.g., Eq. (3), generalized to a matrix–vector product, $\boldsymbol{Z} = \boldsymbol{P} \boldsymbol{A}$) is also Gaussian $\boldsymbol{Z} \sim N(\boldsymbol{\mu}_Z, \boldsymbol{\Sigma}_Z)$. The mean and covariance of vector $\boldsymbol{Z}$ are given by the following:

$$\boldsymbol{\mu}_Z = P \boldsymbol{\mu}_A \tag{5}$$

$$\boldsymbol{\Sigma}_Z = P \boldsymbol{\Sigma}_A P^T \tag{6}$$

More details on the Gaussian uncertainty representation of ODFs can be found in earlier works [28,38] and are not repeated

for brevity. In the stochastic inverse problem, we are required to estimate the uncertainty in the ODF, given statistical constraints on the properties. The unknown ODF values are computed as Gaussian distributions. In our previous work, given k number of total ODF variables, the first $k - 1$ ODF values were modeled to be independent, and the kth ODF was modeled and correlated due to the volume normalization constraint ($q^T A = 1$). The key difference in the Gaussian representation used here is that all k independent nodes are taken to be unknowns, and the normalization constraint is posed as an equality constraint (as described in the next section).

IV. Stochastic Design Optimization with Correlated ODFs

Using the Gaussian representation, a linear system is developed to relate the unknown mean values and covariance matrix elements of the ODF A to the given uncertainty in a set of properties C. The ODFs are modeled as correlated random variables, which lead to a full positive semidefinite symmetric covariance matrix with nonzero entries. The relation between the material properties and the ODF values is defined using the homogenized (volume-averaged) equations as discussed earlier in [31]:

$$p^T A = C \tag{7}$$

In Eq. (7), p is a $(m \times k)$ matrix including the k single crystal values for m properties and denotes the property averaging matrix for C [37].

The linear system solves for mean values of these k ODF parameters and their full $(k \times k)$ symmetric covariance matrix, which is the $n = k + k(k + 1)/2$ number of unknowns in total. The linear system is derived using the ODF normalization constraint ($q^T A = 1$) and homogenized equations for the properties [Eq. (7)]:

$$q^T \mu_A = 1 \tag{8}$$

$$q^T \Sigma_A q = 0 \tag{9}$$

$$p^T \mu_A = \mu_C \tag{10}$$

$$p^T \Sigma_A p = \Sigma_C \tag{11}$$

where Eqs. (8) and (9) show the ODF normalization constraint as applied for the Gaussian distribution. Equation (10) shows the formulation to obtain the vector of mean values of the properties μ_C using the linear transformation rule for Gaussian distribution [Eq. (5)] and the homogenized equation [Eq. (7)]. Equation (11) shows the computation of the covariance matrix for the properties using a linear transformation rule for Gaussians [Eq. (6)].

It is assumed that the mean values of the stiffness parameters μ_C and the stiffness covariance matrix Σ_C are provided. The unknowns of the problem are the ODF mean values vector μ_A and the ODF covariance matrix: Σ_A.

The ODF covariance matrix is expected to agree with the given relation in Eq. (9) because, for any point drawn from the joint ODF probability distribution, the normalization constraint ($q^T A = 1$) should be satisfied. However, this constraint [Eq. (9)] can be enforced by an equivalent constraint derived separately for all rows of the covariance matrix such that

$$\Sigma_A q = 0 \tag{12}$$

The derivation of this constraint is discussed in more detail in the Appendix. Using the preceding formulation, the augmented system of equality constraints for the ODFs can be derived as follows:

$$
\begin{bmatrix}
q^T_{(1 \times k)} & \mathbf{0}_{(1 \times n-k)} \\
p^T_{(m \times k)} & \mathbf{0}_{(m \times n-k)} \\
\mathbf{0}_{(r \times k)} & \bar{P}_{(r \times n-k)} \\
\mathbf{0}_{(k \times k)} & \bar{Q}_{(k \times n-k)}
\end{bmatrix}
\begin{bmatrix}
\mu_{A_{(k \times 1)}} \\
\Sigma_{A^{\text{vec}}_{(n-k \times 1)}}
\end{bmatrix}
=
\begin{bmatrix}
1 \\
\mu_{C_{(m \times 1)}} \\
\Sigma_{C^{\text{vec}}_{(r \times 1)}} \\
\mathbf{0}_{(k \times 1)}
\end{bmatrix}
\tag{13}
$$

where μ_C is the vector of the property mean values (e.g., $\mu^{\text{vec}}_C = [\mu_{C_{11}} \quad \mu_{C_{12}} \quad \mu_{C_{13}} \quad \cdots \quad \mu_{C_{66}}]^T$ for modeling stiffness values of an anisotropic material): Σ^{vec}_C is the vector containing the upper diagonal elements of the symmetric covariance matrix of the following properties: Σ_C such that $\Sigma^{\text{vec}}_C = [\Sigma_{C_{1,1}} \quad \Sigma_{C_{1,2}} \cdots \Sigma_{C_{1,m}} \quad \Sigma_{C_{2,2}} \quad \cdots \quad \Sigma_{C_{2,m}} \cdots \Sigma_{C_{m,m}}]^T$ with a total of $r = m(m + 1)/2$ elements.

Similarly, the upper diagonal entries of the ODF covariance matrix elements are also included in Σ^{vec}_A such that $\Sigma^{\text{vec}}_A = [\Sigma_{A_{1,1}} \quad \Sigma_{A_{1,2}} \cdots \quad \Sigma_{A_{1,k}} \quad \Sigma_{A_{2,2}} \quad \cdots \quad \Sigma_{A_{2,k}} \quad \cdots \quad \Sigma_{A_{k,k}}]^T$.

Note that $\bar{P}$ is the coefficient matrix derived through the covariance relation in Eq. (11) to represent the ODF covariance matrix Σ_A in the vector form Σ^{vec}_A. Likewise, $\bar{Q}$ is the coefficient matrix derived through Eq. (12). The total number of variables n is equal to

$$n = k + \frac{k \cdot (k + 1)}{2}$$

where k shows the number of unknowns of the ODF mean values vector, and $k \cdot (k + 1)/2$ shows the number of unknowns of the symmetric ODF covariance matrix. Therefore, the problem dimensionality is directly dependent on the number of ODF variables k that are used to model the microstructure. The lower bounds of the ODF mean values and variance terms (ondiagonal entries on the covariance matrix) are defined to be zero. The LP problems are solved using an interior-point algorithm.

V. Example Problems

Optimization of the texture of the BCC magnetoelastic alloy galfenol ($Fe_{100-x}Ga_x$) is considered in the examples. The alloy has been shown to exhibit magnetostrictive strains up to 400 ppm in single crystal form (more than 10 times that of α-Fe). Although single crystals of galfenol provide large magnetostriction, their preparation is expensive. Thus, development of polycrystalline galfenol with favorable properties for various applications is desirable. In single crystals of galfenol, the elastic modulus can vary over a large range, from 86 to 260 GPa, depending upon the loading direction. In the rolled sheet form of the alloy, the saturation values of magnetostrictive strains vary as a function of crystal orientation, with the highest strains (attained along the $\langle 001 \rangle$ crystal directions) several times greater than the strains for unfavorable crystal directions. Sensors or actuators in the form of compliant beams of galfenol give the best performance if magnetostriction and strength are maximized. The property matrices for this alloy were calculated based on previous work in [39].

A. Deterministic Nonunique Solutions

Because the linear system developed in the previous section generally corresponds to an underdetermined system of equations, the optimum ODF may not be a unique solution. There might be multiple ODF vectors that can satisfy the prescribed distribution of material properties. To illustrate this, we first identify all possible ODF solutions, given the values of the stiffness parameters

$$[C_{11} \quad C_{12}] = [510.9785 \quad 329.0219] \text{ GPa}$$

using the deterministic solver explained in Ref. [2]. The solver is capable of finding multiple/infinite solutions using the null space of the linear system relating ODF to properties. The infinite solutions are defined as the sum of an initial optimum ODF solution A_1, and solution directions are represented by null space vectors V_i of the coefficient matrix D. The infinite solutions can mathematically be represented as shown in the following:

$$A_i = A_1 + \beta V_i, \quad \text{where } i = 1, 2, 3, 4, \ldots, s \quad (14)$$

$$V_i = \text{Null}(D(:, i)) \quad (15)$$

The number of null space vectors is denoted by s. Even though the number of null space vectors is finite, the number of solutions can be infinite because β can be any number that satisfies the ODF positiveness constraint ($A \geq 0$). Note that the coefficient matrix D also includes the ODF normalization constraint. The null space approach is explained in detail by the authors in Ref. [2]. Using the given input information, we compute the multiple ODF solutions by implementing the null space approach. Each ODF solution identified by the null space approach satisfies the given constraints on the stiffness parameters C_{11} and C_{12}; however, they can provide different values for other material properties. After obtaining the general null space solutions for the stiffness parameters, we solve two different optimization problems. In the first problem, we maximize the magnetostrictive strain λ_{xx} by satisfying the same stiffness criteria that we used to find the null space solutions. The second problem aims to maximize the yield stress σ_y by again satisfying the same prescribed criteria for the stiffness parameters. In Fig. 2, some of the multiple ODF solutions that were identified through the null space approach are shown. These ODF solutions provide the same values of stiffness parameters C_{11} and C_{12}; however, they provide different values for the magnetostrictive strain λ_{xx} and yield stress σ_y as, indicated in Fig. 2. In the next example problems, we will solve the stochastic counterpart of this problem. We find the stochastic ODF solutions, which maximize the mean value of λ_{xx} and σ_y, respectively, given the statistical variations in the stiffness parameters.

B. Stochastic Solution: Maximum Mean Magnetostrictive Strain of a Galfenol Beam

To represent the Gaussian probability distributions, the mean values and covariance matrix of the stiffness parameters C_{11} and C_{12}

are assumed to be provided initially. A full covariance matrix for the ODF increases the problem dimensionality; therefore, a coarser mesh in the Rodrigues domain is employed with 10 ODF nodes. The input parameters for all the application problems are taken as follows:

$$\boldsymbol{\mu}_C = [\mu_{C_{11}} \quad \mu_{C_{12}}]^T = [510.9785 \quad 329.0219]^T \text{ GPa}$$

and

$$\boldsymbol{\Sigma}_C^{\text{vec}} = [\Sigma_{C_{1,1}} \quad \Sigma_{C_{1,2}} \quad \Sigma_{C_{2,2}}]^T = [0.5859 \quad -0.0500 \quad 0.0171]^T \text{ GPa}^2$$

The example problem aims to maximize the mean magnetostrictive strain component of the galfenol beam using the same initially prescribed probability distributions of C_{11} and C_{12}. The ODF solution that provides the maximum value of the mean magnetostrictive strain max $\mu_{\lambda_{xx}}$ will be a subset of the null space solutions shown in Fig. 2. The magnetostrictive strain component to be maximized in this problem is λ_{xx}, and it can be computed using the homogenized equation such that $\lambda_{xx} = \boldsymbol{m}^T A$, where $\boldsymbol{m}$ shows the property vector for the magnetostrictive strain. The objective function of the stochastic LP problem can be defined as follows:

$$\min \boldsymbol{f}^T \boldsymbol{x}$$
$$\boldsymbol{f} = [-\boldsymbol{m}^T(1 \times k) \quad \boldsymbol{0}_{1 \times n-k}]^T$$
$$\boldsymbol{x} = [\boldsymbol{\mu}_{A_{(k \times 1)}} \quad \boldsymbol{\Sigma}_{A_{(n-k \times 1)}}^{\text{vec}}]^T$$

such that Eq. (13) is satisfied:

$$\mu_{A_i} \geq 0, \qquad \Sigma_{A_{ii}} \geq 0$$

The deterministic and stochastic LP problems identify the same optimal value such that max $\lambda_{xx} = 7.3285 \times 10^{-5}$ in the deterministic solution and max $\mu_{\lambda_{xx}} = 7.3285 \times 10^{-5}$ in the stochastic solution.
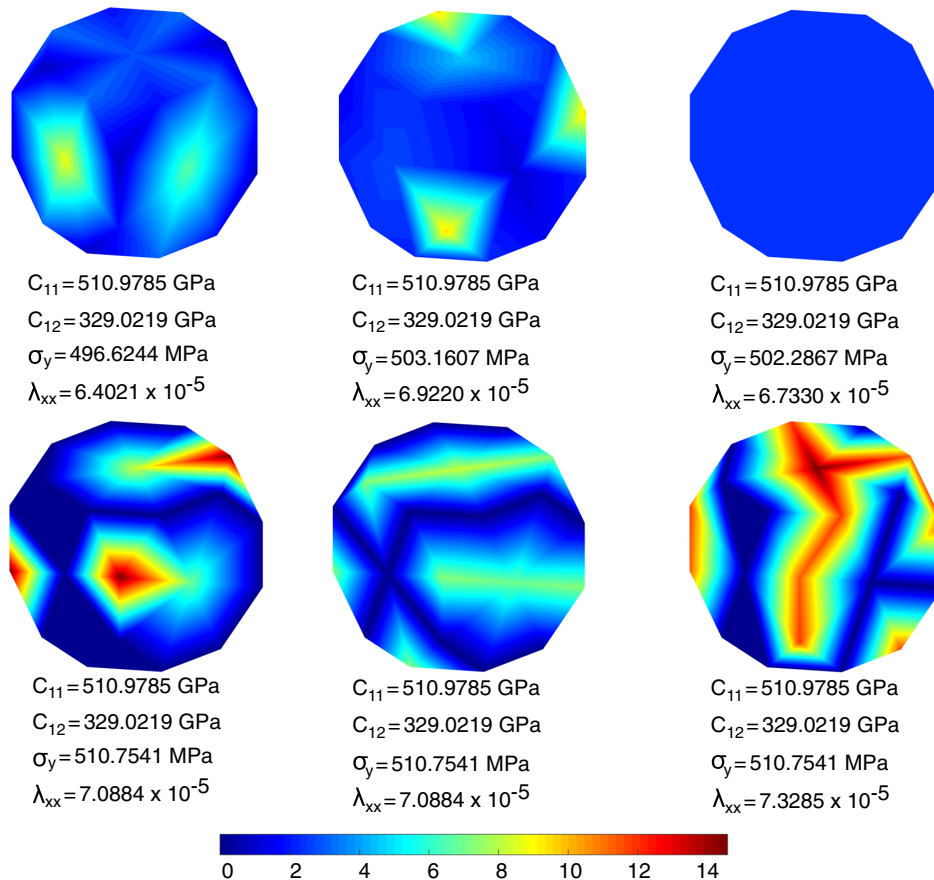

$C_{11} = 510.9785$ GPa
$C_{12} = 329.0219$ GPa
$\sigma_y = 496.6244$ MPa
$\lambda_{xx} = 6.4021 \times 10^{-5}$

$C_{11} = 510.9785$ GPa
$C_{12} = 329.0219$ GPa
$\sigma_y = 503.1607$ MPa
$\lambda_{xx} = 6.9220 \times 10^{-5}$

$C_{11} = 510.9785$ GPa
$C_{12} = 329.0219$ GPa
$\sigma_y = 502.2867$ MPa
$\lambda_{xx} = 6.7330 \times 10^{-5}$

$C_{11} = 510.9785$ GPa
$C_{12} = 329.0219$ GPa
$\sigma_y = 510.7541$ MPa
$\lambda_{xx} = 7.0884 \times 10^{-5}$

$C_{11} = 510.9785$ GPa
$C_{12} = 329.0219$ GPa
$\sigma_y = 510.7541$ MPa
$\lambda_{xx} = 7.0884 \times 10^{-5}$

$C_{11} = 510.9785$ GPa
$C_{12} = 329.0219$ GPa
$\sigma_y = 510.7541$ MPa
$\lambda_{xx} = 7.3285 \times 10^{-5}$

0 2 4 6 8 10 12 14

Fig. 2 Some of the multiple deterministic ODF solutions that satisfy the prescribed values of the stiffness parameters.

However, due to the allowed variations on the stiffness constants, higher or lower values of magnetostrictive strains can be obtained. This is reflected as a Gaussian probability distribution of the magnetostrictive
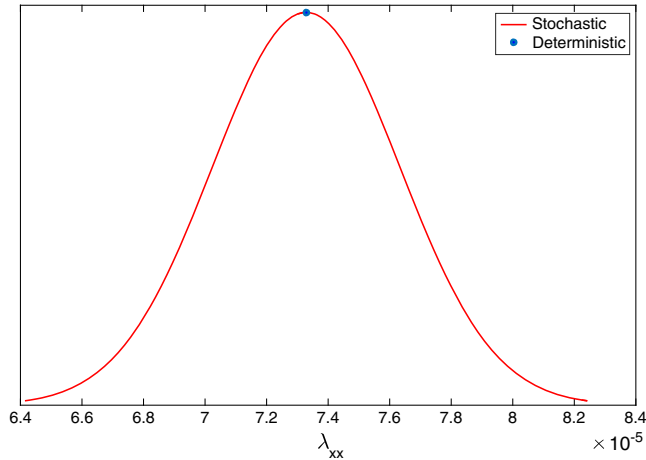

Fig. 3 Magnetostrictive strain distributions of stochastic and deterministic optimization solutions.
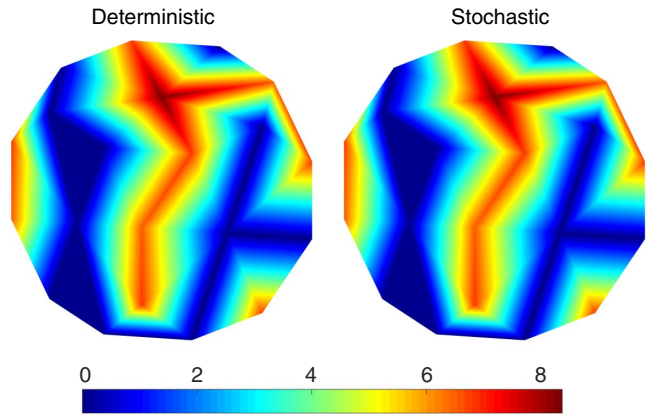

Fig. 4 Comparison of optimum deterministic and stochastic designs for maximum magnetostrictive strain objective.

strain, as seen in Fig. 3. The deterministic and stochastic approaches identify the same solution among all the designs, satisfying the stiffness constraint as shown in Fig. 4. Note that the stochastic ODF solution is illustrated in terms of the ODF mean values. The probability distributions of the optimum ODF solution are shown in Fig. 5. All the ODF values are positive, although the optimal ODF is dominated by nodes 2, 6, 9, and 10. The rest of the independent nodes carry negligible ODF weights. The mean values and standard deviations of the ODF solution in this problem are shown in the orientation space; see Fig. 6. The ODF values with higher mean values also have higher standard deviations.

C. Stochastic Solution: Maximum Mean Yield Stress of a Galfenol Beam

This example problem aims to maximize the mean yield stress of a galfenol beam, given the LP problem formulation in the previous sections. Using the same prescribed probability distributions of the stiffness parameters (C_{11} and C_{12}) as the input, the corresponding ODF probability distributions that also maximize the mean yield stress value are identified. The yield stress can be obtained using the homogenized equation such that $y^T A = \sigma_y$, where y^T shows the property vector for yield stress σ_y. The optimization is again solved for deterministic and stochastic approaches. The objective function of the stochastic LP problem can be defined as follows:

$$f = [-y^T_{(1\times k)} \quad \mathbf{0}_{1\times n-k}]^T \tag{16}$$

The optimum value of the objective function is calculated as follows in the deterministic and stochastic problems:

$$\max \sigma_y = \max \mu_{\sigma_y} = 510.7541 \text{ MPa}$$

The optimum polycrystal solutions of the deterministic and stochastic problem are compared in Fig. 7 (in which a stochastic solution is given in terms of the ODF mean values). The probability distributions of the stochastic optimum ODF design are given in Fig. 8. The optimum yield stress distribution is shown in Fig. 9.

In this problem, the stochastic optimization problem identifies one of the solutions from the null space containing all ODFs with the same maximum yield stress. In Fig. 7, we show another solution (left) that is obtained in the deterministic problem that is not identified as one of the solutions in the stochastic problem. This is because the
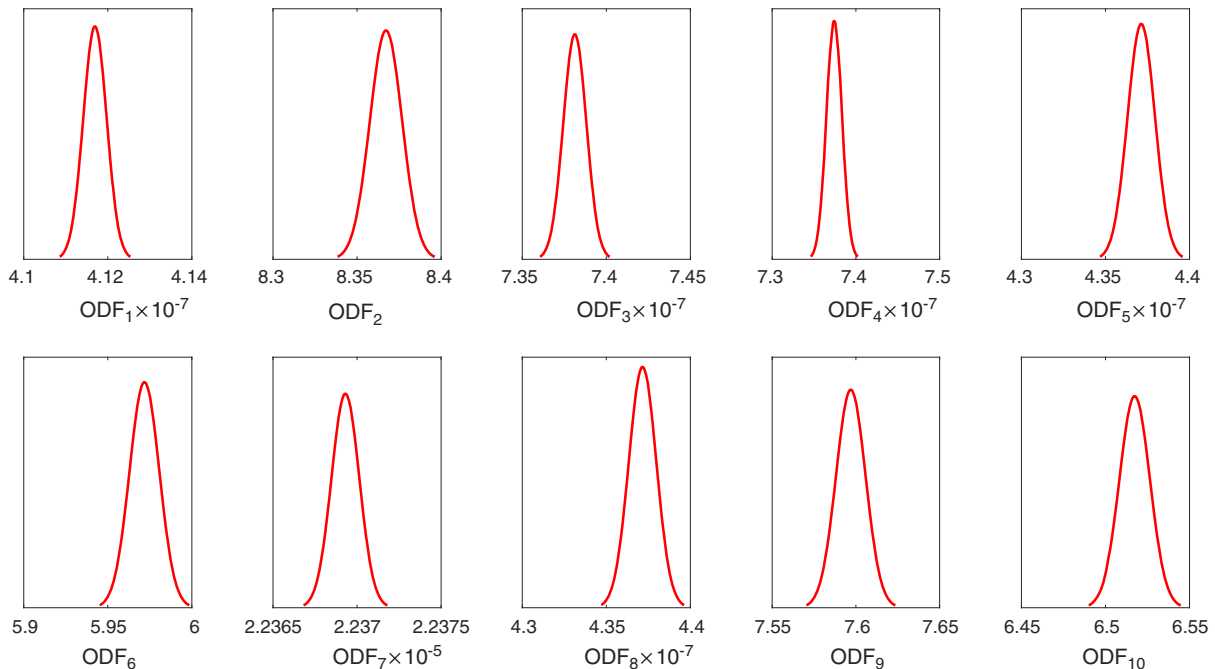

Fig. 5 Probability distributions of the optimum stochastic ODF solution for maximum magnetostrictive strain objective.

a) Mean values of the ODFs   b) Standard deviations of the ODFs
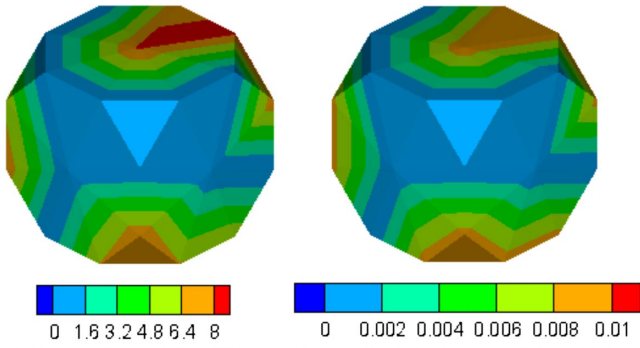
Fig. 6 Statistical features of the optimum ODF probability distributions for the maximum magnetostrictive strain objective.
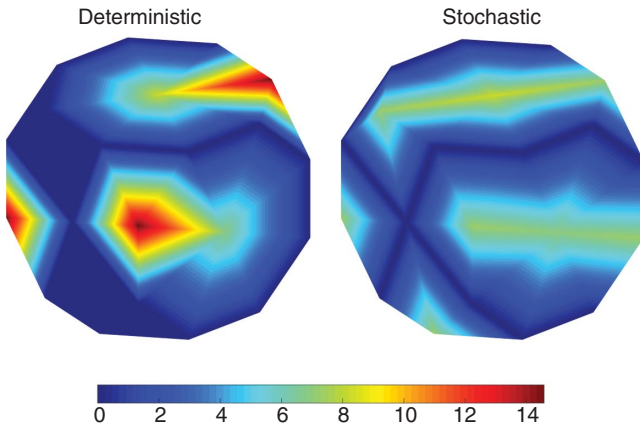

Fig. 7 Comparison of optimum deterministic and stochastic designs for the maximum yield stress objective.

stochastic LP solver is also attempting to match the assigned covariances of the properties, in addition to maximizing the mean yield stress. If the other ODF solution from the deterministic null space solutions is picked, the variances of the stiffness values deviate from the constraint. This difference in the variances between the global stochastic optimum solution and an example null space solution is shown in Fig. 9. Note that the stochastic (null space) plot in Fig. 9 shows the stochastic solution for the yield stress when the mean
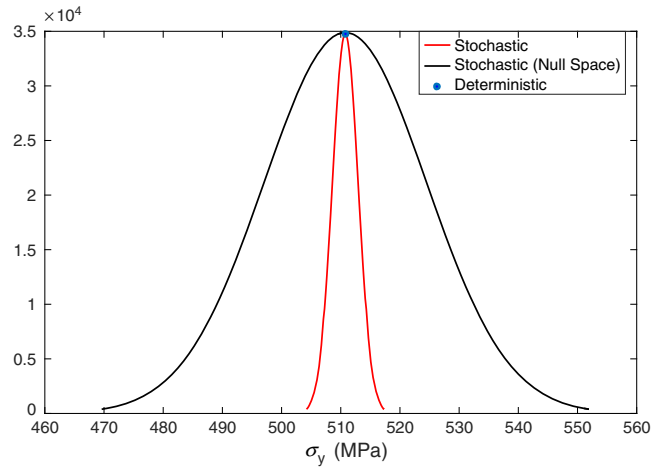

Fig. 9 Yield stress distributions of stochastic and deterministic optimization solutions.

values of the ODFs are taken from a deterministic null space solution that is not the subset of the global stochastic solution. Therefore, the probability distribution looks different than the optimum stochastic result because the null space solutions differ in variance terms when the stochastic problem is solved. The optimum ODF solutions discussed in this paper satisfy positive semidefiniteness for the ODF covariance matrices. The stiffness covariance matrix, which is computed using the optimum ODF solutions, is found to be the same with the initially provided values $\mathbf{\Sigma}_C^{vec}$.

The mean values and standard deviations of the ODF solution are shown in the orientation space; see Fig. 10. The ODF values with higher mean values also have higher standard deviations in this problem.

Note that the probability distributions given in Figs. 5 and 8 satisfy nonnegativity for the ODFs, although Gaussian distributions include negative support. All the variables considered here (i.e., ODFs and the properties) are all positive. Probability density functions (PDFs) with positive variables (e.g., gamma distribution) can instead be considered; however, the only useful analytical result that the authors could find to statistically relate ODFs to properties was the case of the correlated sum of Gamma distribution variables with a constant size parameter [40]. Gaussian methods provide a considerable reduction in computational times as compared to available numerical techniques such as the MCS. Thus, it is recommended that the Gaussian approach presented here be used as a first step before using more advanced inverse UQ models.
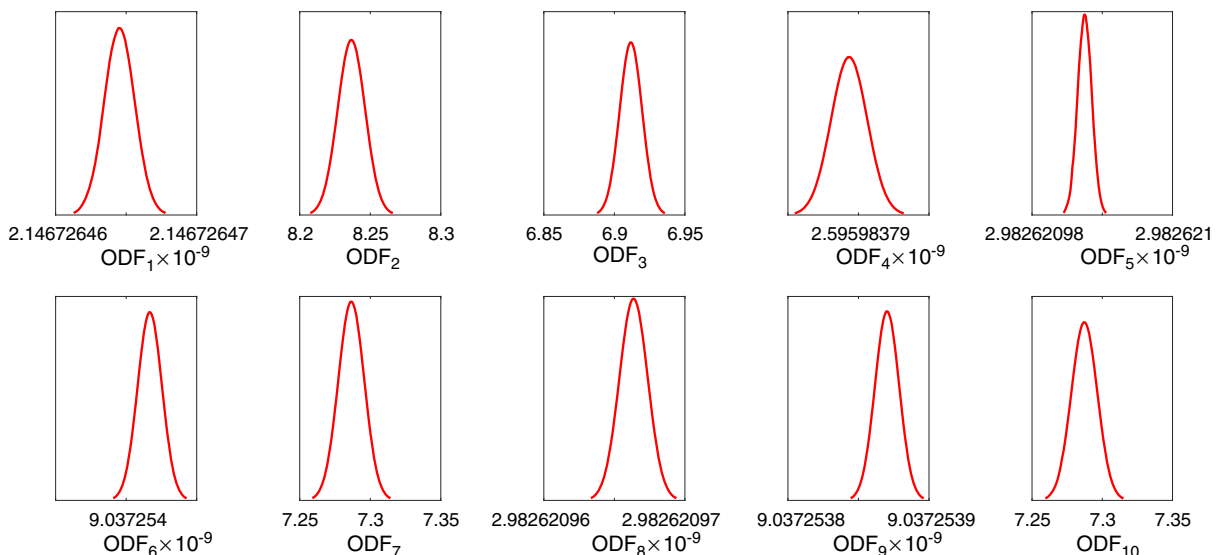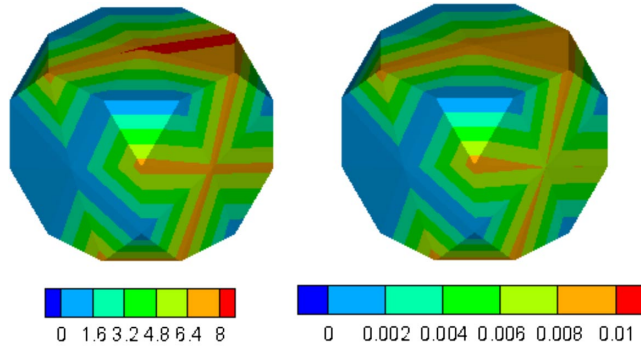

Fig. 8 Probability distributions of the optimum stochastic ODF solution for maximum yield stress objective.

a) Mean values of the ODFs   b) Standard deviations of the ODFs

Fig. 10 Statistical features of the optimum ODF probability distributions for the maximum yield stress objective.

VI. Conclusions

A novel stochastic microstructure optimization methodology is presented that employs an analytical Gaussian uncertainty representation. The microstructure is represented using the ODF, which is discretized using a finite element mesh. Given the probability distributions of a set of material properties, an inverse problem is solved to identify the statistical parameters of microstructures that maximize the mean values of the desired material property. The method takes advantage of the linear relationship between the ODF and properties in the homogenization approach, and the linear transformation rule of Gaussian distributions. The variations in the initially provided material properties are assumed to follow a Gaussian distribution, and the linear transformation feature of the Gaussian distribution is used to solve the ODF probability distributions by defining an inverse LP problem. In the example problems, we use this method to optimize the mean magnetostrictive strains and yield stress of a galfenol alloy, given the stochastic constraints (mean and variances) of two stiffness parameters. It is noted that the deterministic optimization problem results in multiple solutions due to the null space of the coefficient matrix. The stochastic optimization problem can be understood in this context. The Probability Density Function (PDF) of the ODF that results in a given set of stiffness properties is nonunique. There are several solutions to the mean value of the ODF that can result in the desired set of properties. In the formulation, the aim is to identify the PDF that will maximize the mean yield stress, and this will result in a much more constrained solution. In effect, the null space is looked at, and the small set of solutions that leads to the highest mean yield strength is identified. The statistics around one of these solutions was solved for in this example. Having multiple solutions for material design problems is advantageous for manufacturing because it increases the likelihood that one of these textures can be manufactured using a conventional processing technique. Therefore, future effort in this field should focus on integrating processing constraints into this problem.

Appendix: Proof for Covariance Relation

We present that the constraint $q^T \Sigma_A q = 0$ given in Eq. (9) can be enforced strictly by using the new constraint equations defined as $\Sigma_A q = 0$.

Assume that k is the last nodal point, and i represents that any nodal point of the following derivation can be made:

$$\Sigma_{ik} = E[(A_i - \mu_{A_i})(A_k - \mu_{A_k})]$$

where E denotes the expected value operator, A_i and A_k are the ODF values of the ith and kth nodal points, and μ_{A_i} and μ_{A_k} show the mean values for these nodal points:

$$\Sigma_{ik} = E\left[(A_i - \mu_{A_i})\left(\frac{1 - \sum_1^{k-1} A_i q_i}{q_k} - \frac{1 - \sum_1^{k-1} q_i \mu_{A_i}}{q_k}\right)\right]$$

$$\Sigma_{ik} = E\left[(A_i - \mu_{A_i})\left(-\frac{1}{q_k}\left(\sum_1^{k-1} A_i q_i - \sum_1^{k-1} q_i \mu_{A_i}\right)\right)\right]$$

$$-q_k \Sigma_{ik} = E\left[(A_i - \mu_{A_i})\left(\sum_1^{k-1}(A_i - \mu_{A_i})q_i\right)\right]$$

$$-q_k \Sigma_{ik} = \sum_{j=1}^{k-1} q_j \Sigma_{ij}$$

The relation can finally be shown as follows:

$$\sum_{j=1}^{k-1} q_j \Sigma_{ij} + q_k \Sigma_{ik} = \Sigma q = 0$$

References

[1] Acar, P., and Sundararaghavan, V., "Linear Solution Scheme for Microstructure Design with Process Constraints," *AIAA Journal*, Vol. 54, No. 12, 2016, pp. 4022–4031.
doi:10.2514/1.J055247

[2] Acar, P., and Sundararaghavan, V., "Utilization of a Linear Solver for Multiscale Design and Optimization of Microstructures," *AIAA Journal*, Vol. 54, No. 5, 2016, pp. 1751–1759.
doi:10.2514/1.J054822

[3] Kocks, U. F., Tome, C. N., and Wenk, H. R., *Texture and Anisotropy—Preferred Orientations in Polycrystals and Their Effect on Materials Properties*, Cambridge Univ. Press, New York, 2000, pp. 44–77.

[4] Huyse, L., and Maes, M. A., "Random Field Modeling of Elastic Properties Using Homogenization," *Journal of Engineering Mechanics*, Vol. 127, No. 1, 2001, pp. 27–36.
doi:10.1061/(ASCE)0733-9399(2001)127:1(27)

[5] Sakata, S., Ashida, F., Kojima, T., and Zako, M., "Three-Dimensional Stochastic Analysis Using a Perturbation-Based Homogenization Method for Elastic Properties of Composite Material Considering Microscopic Uncertainty," *International Journal of Solids and Structures*, Vol. 45, Nos. 3–4, 2008, pp. 894–907.
doi:10.1016/j.ijsolstr.2007.09.008

[6] Sakata, S., Ashida, F., and Zako, M., "Kriging-Based Approximate Stochastic Homogenization Analysis for Composite Materials," *Computer Methods in Applied Mechanics and Engineering*, Vol. 197, Nos. 21–24, 2008, pp. 1953–1964.
doi:10.1016/j.cma.2007.12.011

[7] Clement, A., Soize, C., and Yvonnet, J., "Computational Nonlinear Stochastic Homogenization Using a Nonconcurrent Multiscale Approach for Hyperelastic Heterogenous Microstructure Analysis," *International Journal for Numerical Methods in Engineering*, Vol. 91, No. 8, 2012, pp. 799–824.
doi:10.1002/nme.v91.8

[8] Clement, A., Soize, C., and Yvonnet, J., "Uncertainty Quantification in Computational Stochastic Multi-Scale Analysis of Nonlinear Elastic Materials," *Computer Methods in Applied Mechanics and Engineering*, Vol. 254, Feb. 2013, pp. 61–82.
doi:10.1016/j.cma.2012.10.016

[9] Creuziger, A., Syed, K., and Gnaupel-Herold, T., "Measurement of Uncertainty in Orientation Distribution Function Calculations," *Scripta Materialia*, Vols. 72–73, Feb. 2014, pp. 55–58.
doi:10.1016/j.scriptamat.2013.10.017

[10] Juan, L., Liu, G., Wang, H., and Ullah, A., "On the Sampling of Three-Dimensional Polycrystalline Microstructures for Distribution Determination," *Journal of Microscopy*, Vol. 44, No. 2, 2011, pp. 214–222.
doi:10.1111/j.1365-2818.2011.03531.x

[11] Hiriyur, B., Waisman, H., and Deodatis, G., "Uncertainty Quantification in Homogenization of Heterogeneous Microstructures Modeled by XFEM," *International Journal for Numerical Methods in Engineering*, Vol. 88, No. 3, 2011, pp. 257–278.
doi:10.1002/nme.3174

[12] Kouchmeshky, B., and Zabaras, N., "The Effect of Multiple Sources of Uncertainty on the Convex Hull of Material Properties of Polycrystals," *Computational Materials Science*, Vol. 47, No. 2, 2009, pp. 342–352.
doi:10.1016/j.commatsci.2009.08.010

[13] Madrid, P. J., Sulsky, D., and Lebensohn, R. A., "Uncertainty Quantification in Prediction of the In-Plane Young's Modulus of Thin Films with Fiber Texture," *Journal of Microelectromechanical Systems*, Vol. 23, No. 2, 2014, pp. 380–390.
doi:10.1109/JMEMS.2013.2279500

[14] Niezgoda, S. R., Yabansu, Y., and Kalidindi, S. R., "Understanding and Visualizing Microstructure and Microstructure Variance as a Stochastic Process," *Acta Materialia*, Vol. 59, No. 16, 2011, pp. 6387–6400.
doi:10.1016/j.actamat.2011.06.051

[15] Zabaras, N., Sundararaghavan, V., and Sankaran, S., "An Information Theoretic Approach for Obtaining Property PDFs from Macro Specifications of Microstructural Uncertainty," *TMS Letters*, Vol. 3, No. 1, 2006, pp. 1–2.

[16] Doltsinis, I., and Kang, Z., "Robust Design of Structures Using Optimization Methods," *Computer Methods in Applied Mechanics and Engineering*, Vol. 193, Nos. 23–26, 2004, pp. 2221–2237.
doi:10.1016/j.cma.2003.12.055

[17] Doltsinis, I., Kang, Z., and Cheng, G., "Robust Design of Non-Linear Structures Using Optimization Methods," *Computer Methods in Applied Mechanics and Engineering*, Vol. 194, Nos. 12–16, 2005, pp. 1779–1795.
doi:10.1016/j.cma.2004.02.027

[18] Besterfield, G. H., Liu, W. K., Lawrence, M. A., and Belytschko, T., "Fatigue Crack Growth Reliability by Probabilistic Finite Elements," *Computer Methods in Applied Mechanics and Engineering*, Vol. 86, No. 3, 1991, pp. 297–320.
doi:10.1016/0045-7825(91)90225-U

[19] Burr, V. D. T., Sudicky, E. A., and Naff, R. L., "Nonreactive and Reactive Solute Transport in Three Dimensional Heterogenous Porous Media: Mean Displacement, Plume Spreading and Uncertainty," *Water Resources Research*, Vol. 30, No. 3, 1994, pp. 791–815.
doi:10.1029/93WR02946

[20] Rahman, S., and Kim, J. S., "Probabilistic Fracture Mechanics for Nonlinear Structures," *International Journal of Pressure Vessels and Piping*, Vol. 78, No. 4, 2001, pp. 261–269.
doi:10.1016/S0308-0161(01)00006-0

[21] Grigoriu, M., Saif, S., El-Borgi, M. T. A., and Ingraffea, A., "Mixed-Mode Fracture Initiation and Trajectory Prediction Under Random Stresses," *International Journal of Fracture*, Vol. 45, No. 1, 1990, pp. 19–34.
doi:10.1007/BF00012607

[22] Matous, K., Geers, M. G. D., Kouznetsova, V. G., and Gillman, A., "A Review of Predictive Nonlinear Theories for Multiscale Modeling of Heterogeneous Materials," *Journal of Computational Physics*, Vol. 330, Feb. 2017, pp. 192–220.
doi:10.1016/j.jcp.2016.10.070

[23] Redeker, M., and Haasdonk, B., "A POD-EIM Reduced Two-Scale Model for Crystal Growth," *Advances in Computational Mathematics*, Vol. 41, No. 5, 2015, pp. 987–1013.
doi:10.1007/s10444-014-9367-y

[24] Kerfriden, P., Rodenas, J., and Bordas, S., "Certification of Projection-Based Reduced Order Modelling in Computational Homogenisation by the Constitutive Relation Error," *International Journal for Numerical Methods in Engineering*, Vol. 97, No. 6, 2014, pp. 395–422.
doi:10.1002/nme.v97.6

[25] Abdulle, A., and Henning, P., "A Reduced Basis Localized Orthogonal Decomposition," *Journal of Computational Physics*, Vol. 295, Aug. 2015, pp. 379–401.
doi:10.1016/j.jcp.2015.04.016

[26] Hernandez, J. A., Oliver, J., Huespe, A. E., Caicedo, M. A., and Cante, J. C., "High-Performance Model Reduction Techniques in Computational Multiscale Homogenization," *Computer Methods in Applied Mechanics and Engineering*, Vol. 276, July 2014, pp. 149–189.
doi:10.1016/j.cma.2014.03.011

[27] El Halabi, F., Gonzalez, D., Chico, A., and Doblare, M., "FE^2 Multiscale in Linear Elasticity Based on Parametrized Microscale Models Using Proper Generalized Decomposition," *Computer Methods in Applied Mechanics and Engineering*, Vol. 257, April 2013, pp. 183–202.
doi:10.1016/j.cma.2013.01.011

[28] Acar, P., and Sundararaghavan, V., "Uncertainty Quantification of Microstructural Properties due to Variability in Measured Pole Figures," *Acta Materialia*, Vol. 124, Feb. 2017, pp. 100–108.
doi:10.1016/j.actamat.2016.10.070

[29] Adams, B. L., Henrie, A., Henrie, B., Lyon, M., Kalidindi, S. R., and Garmestani, H., "Microstructure Sensitive Design of a Compliant Beam," *Journal of the Mechanics and Physics of Solids*, Vol. 49, No. 8, 2001, pp. 1639–1663.
doi:10.1016/S0022-5096(01)00016-3

[30] Kalidindi, S. R., Houskamp, J., Lyons, M., and Adams, B. L., "Microstructure Sensitive Design of an Orthotropic Plate Subjected to Tensile Load," *International Journal of Plasticity*, Vol. 20, Nos. 8–9, 2004, pp. 1561–1575.
doi:10.1016/j.ijplas.2003.11.007

[31] Liu, R., Kumar, A., Chen, Z., Agrawal, A., Sundararaghavan, V., and Choudhary, A., "A Predictive Machine Learning Approach for Microstructure Optimization and Materials Design," *Nature Scientific Reports*, Vol. 5, June 2015, Paper 11551.
doi:10.1038/srep11551

[32] Sundararaghavan, V., and Zabaras, N., "A Statistical Learning Approach for the Design of Polycrystalline Materials," *Statistical Analysis and Data Mining*, Vol. 1, No. 5, 2009, pp. 306–321.
doi:10.1002/sam.v1:5

[33] Sundararaghavan, V., and Zabaras, N., "On the Synergy Between Texture Classification and Deformation Process Sequence Selection for the Control of Texture-Dependent Properties," *Acta Materialia*, Vol. 53, No. 4, 2005, pp. 1015–1027.
doi:10.1016/j.actamat.2004.11.001

[34] Taylor, G. I., "Plastic Strain in Metals," *Journal of the Institute of Metals*, Vol. 62, May 1938, pp. 307–324.

[35] Kumar, A., and Dawson, P. R., "Computational Modeling of F.C.C. Deformation Textures over Rodrigues' Space," *Acta Materialia*, Vol. 48, No. 10, 2000, pp. 2719–2736.
doi:10.1016/S1359-6454(00)00044-6

[36] Sundararaghavan, V., and Zabaras, N., "A Multi-Length Scale Sensitivity Analysis for the Control of Texture-Dependent Properties in Deformation Processing," *International Journal of Plasticity*, Vol. 24, No. 9, 2008, pp. 1581–1605.
doi:10.1016/j.ijplas.2007.12.005

[37] Sundararaghavan, V., and Zabaras, N., "Linear Analysis of Texture-Property Relationships Using Process-Based Representations of Rodrigues Space," *Acta Materialia*, Vol. 55, No. 5, 2007, pp. 1573–1587.
doi:10.1016/j.actamat.2006.10.019

[38] Acar, P., Srivastava, S., and Sundararaghavan, V., "Stochastic Design Optimization of Microstructures with Utilization of a Linear Solver," *AIAA Journal*, Vol. 55, No. 9, 2017, pp. 3161–3168.
doi:10.2514/1.J056000

[39] Kumar, A., and Sundararaghavan, V., "Simulation of Magnetostrictive Properties of Galfenol Under Thermomechanical Deformation," *Finite Elements in Analysis and Design*, Vol. 127, May 2017, pp. 1–5.
doi:10.1016/j.finel.2016.11.009

[40] Alouini, M. S., Abdi, A., and Kaveh, M., "Sum of Gamma Variates and Performance of Wireless Communications Systems over Nakagami Fading Channels," *IEEE Transactions on Vehicular Technology*, Vol. 50, No. 6, 2001, pp. 1471–1480.
doi:10.1109/25.966578

R. Ohayon
Associate Editor